Journal of Materials Chemistry B

Accepted Manuscript

ROYAL SOCIETY OF CHEMISTRY

www.rsc.org/materialsB

Journal Name

RSCPublishing

ARTICLE

A novel chitosan-collagen–based hydrogel to use as dermal filler: initial *in vitro* and *in vivo* investigations

Cite this: DOI: 10.1039/x0xx00000x

Received ooth January 2012,
Accepted ooth January 2012

DOI: 10.1039/x0xx00000x

www.rsc.org/

Xiaoxuan Ma[1,2,§], Jianjun Deng [1,2,§], Yuzhang Du [1,2,§], Xian Li [1,2,§], Daidi Fan[1,2,*], Chenhui Zhu[1,2], Junfeng Hui[1,2], Pei Ma[1,2], Wenjiao Xue[3]

The novel hydrogels (termed HCD hydrogels) were synthesized based on human-like collagen (HLC) and chitosan (CS) cross-linked with dialdehyde starch (DAS). The biological stability and biocompatibility of HCD hydrogels were determined through *in vitro* and *in vivo* tests. The mechanism of hydrogel formation using Fourier transform infrared spectroscopy (FTIR), which showed that covalent bonds formed via acetalization and Schiff base reactions. Biological stability was evaluated *in vitro* by degrading HCD hydrogels with class I collagenase, class II collagenase, and both class I and class II collagenases and *in vivo* after subcutaneously injecting HCD into animal model. The biocompatibility of HCD hydrogels was studied by two methods: (i) MTT and cytomorphology cytotoxicity and cytocompatibility and (ii) *in vivo*, whereby histomorphometry, transmission electron microscopy (TEM), and immunohistochemistry were used to compare different types of surgically introduced hydrogels-our HCD hydrogels, SunMax Collagen Implant hydrogels (SUM hydrogels), and OUTLINE & EVOLUTION Injectable Synthetic Gel hydrogels (EVL). The *in vivo* analyses were performed at 1, 9, 12, and 28 weeks after surgery. The hydrogel biodegradation results showed that the normalized residual weight (W_R) of HCD hydrogels varied with DAS content. *In vitro*, we found that the minimum W_R of HCD hydrogels was 42.19% after 28 weeks when degraded by both types of class I and class II collagenase. The MTT assay indicated that the minimum relative growth rate of cells (RGR) was 93% after they were incubated with HCD hydrogels for 7 days, suggesting good cytocompatibility. *In vivo* histomorphometry results indicated that HCD hydrogels effectively filled tissue voids and did not cause redness, edema, festering, or color changes. In addition, a few vessels grew into the hydrogel and a thin fibrous capsule was eventually produced. TEM and immunohistochemistry studies suggested that HCD hydrogels produced less intense inflammatory responses than those produced by SUM hydrogel and EVL hydrogel. Overall, HCD hydrogels afford both enhanced biological stability and excellent biocompatibility, making them potentially promising for skin patch scaffolds, wrinkle treatments, and tissue cavity fillers.

Keywords: biology stability, biocompatibility, covalentcross-linking, dermal filler, hydrogel

Introduction

Injectable hydrogels, which offer minimally invasive delivery and low injection costs, are promising scaffolds for cell encapsulation, drug delivery, tissue repair, and reconstructive surgery. [1, 2] While injectable hydrogels may be well suited to tissue repair, they must also be biocompatible, biologically stable, and have a nontoxic initiating system. Therefore, hydrogels are usually fabricated using a suitable cross-linker to create covalent bonds between natural biomacromolecules (*i.e.*, collagen, chitosan, alginate, and hyaluronan), such that they retain their biocompatibility in cross-linked form.

Collagen is an especially useful biomaterial because it has excellent biocompatibility, it is naturally degradable, and it produces a weak immune response.[3] Because of these characteristics, collagen has become a primary material for skin grafts,[4] artificial bones,[5] and artificial blood vessels.[6] It is even used in collagen sponge devices, which help control bleeding during surgical operations.[7] Human-like collagen (HLC) is

highly expressed by recombinant *Escherichia coli* BL21 that contains a partial cDNA clone derived from human collagen mRNA.[8] HLC has been used in research on injectable hydrogels,[9] artificial bone,[10] and vascular scaffolds[11] because it is water soluble, biodegradable, biocompatible, and it has low immunogenicity.

Chitosan (CS), also known for being biocompatible, biodegradable, and only weakly immunogenic, is metabolized by certain human enzymes such as lysozyme.[12] Consequently, chitosan is often used for topical ocular applications, implantations, and injections.[13]

Biomacromolecules like collagen and chitosan are often incorporated into hydrogels and examined for additional medical applications. Hydrogel networks can be created through entanglements, covalent bonds, or secondary interactions.[14] Biologically stable hydrogels with a strong network structure are generally synthesized through covalent crosslinking, which forms irreversible chemical bonds. For such networks to form bridges between polymeric chains are established by cross-linkers that have at least two reactive functional groups.[13] Dialdehydes such as glyoxal and glutaraldehyde have previously been used to covalently cross-link hydrogels, given that acetalization and schiff base reactions occur between hydroxyl/amino groups and aldehyde groups. However, many studies have shown that glutaraldehyde is a neurotoxin, even though its fate in the human body is not fully understood, and glyoxal is mutagenic.[15,16]

Dialdehyde starch (DAS), which has two reactive functional groups (aldehyde groups) in each glucose unit, was used as the cross-linking agent in our study. DAS is produced by periodate-controlled oxidation of the C-2 and C-3 bonds of native starch's anhydroglucose units.[17,18] DAS that has a low degree of oxidation could potentially be used in foods and biomaterials because it may be more biocompatible and less toxic than highly oxidized DAS.[19] In a previous study, the acute oral toxicity of DAS was evaluated in rats; the study found that when 40% of its glucose units were oxidized, DAS (5% wt of the fabricated hydrogels.) permitted normal growth.[18, 19] Therefore, we chose to synthesize our hydrogels, using DAS with 30% of its glucose units oxidized (DAS-30) and at a concentration of 0.5% to 1.5% (wt.).

The chitosan/collagen based hydrogels were report by Xian Li[9, 20-24], the EDC and the β-Gp as cross-linking agent to form the injectable hydrogels. Because the EDC have the toxicity, and the residue of EDC in hydrogels is difficulty to handle as the super hand problems. The CCG hydrogel, β-Gp as cross-linking agent and the CCAG hydrogel using self-assemble technique is hot spot in the latest research, which the fibers inside the hydrogel pores reduced the quantity of macrophages, decreased the degree of inflammation, and improved the anti-degradation of the modified hydrogels. However, the Cytocompatibility of hydrogels is still need a novel test method to study toxicologist. In addition, dialdehyde starch (DAS) as cross-linking agent is a novel crosslinker not previously described and therefore they are new.

Therefore, the main purpose of this study was to prepare hydrogels with enhanced biological stability and good biocompatibility and decreased the toxicity. To accomplish this, we designed a formulation scheme in which DAS was used to covalently cross-link HLC and CS, producing HCD hydrogels.

Materials and methods

Materials

HLC was expressed by *E. coli* with a cloned partial cDNA reversed from the mRNA coding for human collagen[8] (Chinese patent number: ZL01106757.8). The required CS (molecular weight 5.5×10^5, deacetylation degree 90–92%) was supplied by Qingdao Ocean Co., Ltd (China). DAS (molecular weights 3.2×10^6 and degree of oxidation was 1%) was purchased from Sigma-Aldrich (Shanghai) Trading Co., Ltd. OUTLINE&EVOLUTION Injectable Synthetic Gel (I) (EVL) (Product standard No YZB/FRC 0795-^{20}05) was purchased from ProCytech S.A.S France. Sunmax Collagen Implant I (SUM) (Product standard No YZB/State (Taiwan) 0389-2009 Collagen Implant) was purchased from SunMax Biotechnology CO., Ltd. The mice as the animals models were provided by Xi'an Jiaotong University, and all solvents and reagents were analytical grade.

Fabrication of the HCD hydrogels

HLC was dissolved in ultrapure water to prepare 4% (w/v) solution, and 2% (w/v) CS was obtained by dissolving CS in 1% (v/v) acetic acid solution, then, the 4% HLC/2%CS (2:1 v/v) mixture with pH=7.4 was prepared by adding 2% (w/v) CS to 4% HLC. The DAS with the ultrapure water were heated at 90℃ for 60 minutes to prepare 2% (w/v) DAS liquor with pH=7.4. The following procedures were manipulated in aseptic condition for getting sterile gels. The aseptic 4% HLC/2%CS mixture (pH=7.4) and 2% DAS aseptic solution (pH=7.4) were prepared by 0.22μm filter. The next, the aseptic HLC/CS mixture and sterile DAS solution were matched according to Table 1 to fabricate various hydrogels.

Table 1. Compositions of the HCD hydrogels with different DAS contents

Hydrogels name	*HLC/CS (mL) a*	*DAS (mL) b*	*Ultrapure water (mL)*
HCD-1.5	3.5	1.5	0
HCD-1.0	3.5	1.0	0.5
HCD-0.5	3.5	0.5	1.0

a sterile mixture of 4% HLC/2%CS (2:1 v/v) (pH=7.4)

b sterile 2% (w/v) DAS liquor (pH=7.4)

Fourier transforms infrared spectroscopy (FT-IR)

FT-IR spectra of the HLC, CS, DAS, and HCD-1.0 hydrogel were recorded using a Perkin Elmer Spectrum 2000 spectrometer (Perkin-Elmer Instrument, Inc.) in the range of

4000-600 cm-1. Each spectrum was taken as the average of 16 scans at a resolution of 4 cm-1.

Swelling measurement

For the swelling studies, dried gels were placed in triplicate in physiological saline at various times to reach equilibrium, after which the gels were weighed. The equilibrium swelling ratio was given as $(W_s-W_d)/W_s$, where W_s and W_d represent the weight of swollen gel and the dried gel, respectively.

Compression Experiment

The hydrogels were tested by a gel strength instrument (Electronic Universal Testing Machine) as follows: firstly, the height of the compression plate was adjusted to 10 mm and its final height was adjusted to 4 mm. The disc of instrument was circular with a diameter of 10 mm and the compression speed was adjusted to 2 mm/min. The gel was cut to a length of 10 mm and placed on the instrument disc. When the compression displacement reached 6 mm, the test was stopped. The compression modulus and the relationship between the compression stress and compression displacement were calculated.s

Hydrogels Sterilization

HCD Hydrogels were prepared by the sterile of HLC, CS and DAS. The specific ratio was same as Table 1. The operation process is done in the v aseptic work station. The lyophilization procedure is: 1), prepared HCD hydrogels in centrifugal tube were freeze in 80□ at 3h; 2), the freeze HCD hydrogels were placed in lyophilizer more than 48h after the temperature lower than -58℃; 3), the dried HCD hydrogels were taken out and cut to a length of 1 mm. And then the samples were sterilized by gamma irradiation or non-gamma irradiation. In order to assess the gamma rays may affect polymers and particularly soft samples of natural origin. The weight loss of HCD hydrogels after degradation by physiological saline was measured.

Biodegradation in vitro

The biodegradation *in vitro* was assessed by collagenase: 100U/mL class I (300 U/mg, Sigma), 100 U/mL class II (350 U/mg, Sigma) and class I + II (1:1 v/v). After weighed and sterilized by Co^{60} gamma irradiation , the dried gels samples (W_0) (n=3) were transferred to 24-well culture plate, and 1.5 mL the enzyme buffer was filled in the well of 24-well culture plate which was kept static at 37.0±0.5℃ in an incubator. After soaking for 4, 8, 12, 16, 20, 24, and 28 weeks, the samples were withdrawn from the enzyme buffer and immediately lyophilized and then weighed again (W_1). Weight residual rate (W_R) was calculated according $W_R=W_1/W_0\times100\%$. This process was applied to three parallel samples, the mean value of weight residual$W_{R0}=(W_{R1}+W_{R2}+W_{R3})/3$ was calculated. Where W_{R1}, W_{R2}, and W_{R3} were the weight residual rate of each parallel samples, respectively.

Structure of DAS hydrogels before/after biodegradation in vitro

Observations of morphologies and pore structures of the DAS hydrogels before assessment and after 28 weeks biodegradation were made using scanning electron microscopy (SEM) at 20 kV (JEOL JSM-6400). Characterizations of the microstructure in dried samples were performed. Prior to the observation, specimens were immersed into liquid nitrogen, fractured, and then sputtered with a thin layer of gold.

Cytocompatibility analysis

MTT ASSAY OF HCD HYDROGELS' EXTRACT SOLUTION

Two kinds of cells were used, one was chondrocytes isolated from the cartilage tissue of rabbit ears as the reference[10] and the other was baby hamster kidney cells (BHK21). In a CO_2 (5%) incubator at 37℃, BHK-21 and chondrocytes were cultured in RPMI Medium 1640 (1640) and Dulbecco's Modified Eagle Medium (DMEM) (GIBCO™, Invitrogen Corporation) with 10% (v/v) fetal bovine serum (FBS) for 24–36 hours, respectively. The medium was changed every two days and the cells of passages 3–6 were used in the following studies.
The long about 6 mm hydrogels were transferred to the well of 24-well culture plate with filling 1 mL DMEM containing 10% (v/v) FBS and cultured for 24 hours at 37℃ in the incubator. After that, the medium was deemed as 100% extract solution. According the standardization, 50% extract solution need to be prepared also. The 1×10^4 mL^{-1} cells suspension were seeded to the well of 96-well culture plate with 100μl per well (n=6) and then cultured in the incubator for 24 hours in order to make cell attached the bottom of the culture plate. Then, cell medium was removed, and each well of the culture plate was filled with 100μl 100% or 50% extract solution. After incubation for 1 day, 3, 5, and 7 days, the dishes were analysed for the relative growth rate (RGR) with Cell Counting Kit-8 (CCK-8, SAB) following the manufacturer's manual. The relative growth rate (RGR) was calculated as: $RGR=[OD]_{test}/[OD]_{control}\times100\%$, $[OD]_{test}$ and $[OD]_{control}$ were the mean value of six parallel of absorbance in the extract solution and blank sample (culture medium), respectively.

SEEDING OF CELLS ON THE HCD HYDROGELS

BHK-21 was acted as the cell model for this assessment. The samples, which were prepared by cutting HCD into slices with the thickness approximate 1mm, were shifted to the well of 24-well culture plate and 1mL 3×10^4 mL^{-1} cells suspension of BHK-21 was seeded to each well (n=6). For the sample was thin and hyaline, so we could directly compare the cellular morphology and proliferation between test and blank samples by the Inverted Microscope with CCD camera (Nikon Eclipse 80i) after incubation for 1 day, 3, 5, and 7 days.

SEM OBSERVATION OF THE CELLS/DAS HYDROGELSCONSTRUCTS

After gross appearance with the Inverted Microscope with CCD camera, the cellular morphology in the DAS-1.0 hydrogel was evaluated by SEM. The cells/DAS-1.0 hydrogels samples were fixed using 2.0% glutaraldehyde in cacodylate/saccharose

buffer (0.05 M/0.3 M, pH 7.4) for 4 h at 4℃. Following fixation, samples were washed three times in cacaodylate/saccharose buffer (0.05 M/0.3 M, pH 7.4) and dehydrated through successive raising concentration ethanol baths from 70% to 100% alcohol. Then, samples were dried in a critical point dryer and gold sputtered for analysis. Samples were observed with JEOL JSM-6400 SEM operating at 20 kV.

HISTOCOMPATLBILITY ASSESSMENT *IN-VIVO* SURGICAL PROCEDURE

All animal experiments were conducted in accordance with the committee guidelines of the Northwest University for animal experiments, which, in turn, meet the NIH guidelines for the care and use of laboratory animals. In view that the material must be an injectable hydrogel with strong mechanical strength, HCD-1.0 was chosen for further study, and OUTLINE&EVOLUTION Injectable Synthetic Gel (I) ® ((EVL). ProCytech S.A.S France) and Sunmax Collagen Implant I ® ((SUM). SunMax Biotechnology CO., Ltd. Taiwan) were deemed as control groups. In this investigation, 36 mice provided by Xi'an Jiaotong University (age 8 weeks, weight 30±5 g) were random divided into two groups (group I and group II) with 18 animals per group (female and male half-and-half) and fed the animals at controlled temperature of 20-22℃ and relative humidity of 50-60% for 7 days before surgery. Hairs on dorsum were removed by depilatory and a 4×4 cm nakedness region was obtained before operation. Vertebral column of the mice was regarded as boundary, group I, 0.2 mL of the HCD-1.0 was injected subcutaneously into left side and the same dose of SUM was injected subcutaneously into right side by 1 mL syringe. The groupII, 0.2 mL of HCD-1.0 and EVL was injected subcutaneously into left and right side, respectively (n=3).

HISTOMORPHOMETRY EVALUATION

Mice were moulted once again before the assessments and sacrificed after 1 week, 9, 12, and 28 weeks surgery. The following parameters of the injected site were evaluated by gross appearance with digital camera (Nikon TE2000-U) (n=3): the gels' color and mechanical strength, redness, edema, fester, vessels, and the fiber capsule. After gross appearance, the implant/tissue constructs were harvested and cut into half, one half for TEM evaluation and the other for immunohistochemistry analysis.

TRANSMISSION ELECTRON MICROSCOPY (TEM) FOR INFLAMMATORY RESPONSES EVALUATION

To gain further insight into the inflammatory responses level of HCD-1.0 compared with the control groups post-surgery, studying the cell types and quantities of the inflammatory cells based on pathology is a very necessary and effective method. In TEM assessment, the samples (n=3) were fixed immediately with 2.5% phosphate buffered glutaraldehyde for overnight, rinsed in 0.1 M PBS for 30 minutes, dehydrated through a series of gradient ethanol (30%, 50%, 70%, 90%, 95% and 100%) for 20 minutes at each concentration, postfixed in 0.5% osmium tetroxide for 4 hours, and rinsed for 10 minutes using a 0.1 M PBS again. Next, samples were dehydrated with 80% acetonitrile (20minutes), 90% acetonitrile (20minutes), 100% acetonitrile (20minutes), and then displaced by epoxyethane. Ultrathin sections (50–70 nm)were cut and stained with 4% uranyl acetate and 0.5% lead citrate for observation by TEM (HITACHI, H-600, Japan).

IMMUNOHISTOCHEMISTRY FOR INFLAMMATORY RESPONSES EVALUATION

In the immunohistochemistry analysis, the samples (n=3) were immediately fixed in 10% neutral buffered formalin for overnight. The next, they were rinsed in 0.1 M PBS for 30 minutes to remove residual formalin, dehydrated through a series of gradient ethanol for 15 minutes at each concentration, immersed in liquid wax for overnight, and then embedded in epoxy resin. Blocks were sectioned using a Leica RM2235 thin semiautomatic microtome (Leica Instruments Ltd, Germany) with 4 μm thickness. Using anti-mouse CD4 (ABCam, UK), CD8 (ABCam, UK) and CD68 (ABCam, UK) as the primary antibodies assessed the inflammatory responses. Endogenous peroxidase activity and non-specific binding was blocked by incubation with 1% (v/v) hydrogen peroxide in methanol and 10% (v/v) goat serum in TBS for 20 min at room temperature, respectively. Samples were incubated with anti-mouse CD4, CD8, and CD68 anti-body for 1 hour at room temperature. Then, the sections coated by primary antibodies were incubated in HRP-labeled (Sigma Aldrich, US) for 30 minutes in a 37℃ chamber. Images were acquired using an optical microscope connected to a CCD camera (Nikon Eclipse 80i).

Statistical analysis

Data are expressed as mean ±SD. Analysis was performed using the Statistical Program for Social Science (SPSS) for Windows. Results were made using student's T-test (two tail, unequal variance) and analysis of variance (ANOVA). A p-value of <0.05 was considered to be statistically significant.

Result and discussion

Fourier transforms infrared spectroscopy (FTIR) of the macromers

Fourier transform infrared spectroscopy (FTIR) was used to track the formation of HCD hydrogels. The FTIR spectra of the HLC, CS, and DAS macromers and the HCD-1.0 hydrogel are shown in Fig. 1 as curves a, b, c, and d, respectively. The peaks at 1664 cm^{-1} and 1630 cm^{-1} corresponding to the amide I ($\nu_{(C=O)}$) and amide II of ($\delta_{(N-H)}$ and $\nu_{(C-N)}$) of RCONHR' are clearly seen in curve a, and these are the characteristic peaks of HLC. The peaks corresponding to the amide I ($\nu_{(C=O)}$) and amide II ($\delta_{(N-H)}$ and $\nu_{(C-N)}$) of CS, which exist at 1643 cm^{-1} and 1586 cm^{-1}, and the characteristic peak of $\nu_{(N-H)}$ at 3433 cm^{-1}, which corresponds to $-NH_2$ and overlaps with the $\nu_{(O-H)}$ peak, are clearly seen in curve b. These peaks are considerably weakened

after the HCD-1.0 hydrogel formed, as can be seen in when comparing curve b with d. This confirms that the amino group participated in the reaction. In curve c, the peaks at 2813 cm^{-1} and 2700 cm^{-1},corresponding to the Fermi resonance of $\nu_{(C-H)}$, and the characteristic peak of $\nu_{(C=O)}$ at 1738 cm^{-1} demonstrate the existence of the aldehyde group in DAS, but these characteristic peaks are absent in curve d after the HCD-1.0 hydrogel formed. At the same time, curve d shows a new peak associated with $\nu_{(C=N)}$ at 1646 cm^{-1} and four new peaks between 1150 cm^{-1} and 1025 cm^{-1} associated with the vibrational coupling from the two C−O−C groups. These results demonstrate that we successfully synthesized HCD hydrogels via the Schiff base and acetalization reactions (see Fig.2).

Mechanism for fabricating HCD hydrogels

The cross-linking mechanism for HCD hydrogels is shown in Fig. 2. The chitosan monomer possesses two hydroxyl groups and an amino group on a glucosamine ring (Fig. 2 A), while the dialdehyde starch monomer contains two carbonyl groups (Fig. 2 B). The basic structure of the human-like collagen (HLC) polypeptide chain is shown in (Fig. 2 C). A structural prerequisite for the HLC polypeptide chain is that a glycine residue,[25, 26] the smallest amino acid, is present in every third position of the polypeptide chains. The resulting $(Gly\text{-}X\text{-}Y)_n$ repeat structure is characteristic of all collagen molecules. Depending on the collagen type, specific proline and lysine residues are modified by post-translational enzymatic hydroxylation[27], but for most collagen types, hydroxyproline and proline often occupy the X and Y positions. For the HCD gels, hydroxyproline, lysine, and basic amino acid residues provided the hydroxyl and/or amino groups through which the main covalent bonds were formed.

Carbonyl groups can react with imines due to the presence of the amino groups on HLC and CS, which add to aldehyde groups on the DAS cross-linker to form a Schiff base (Fig. 2 D). Because the carbon of the carbonyl group is located in the sp^2 orbital, it is easily hybridized by the other three atoms lying in the same plane, such that the bond angles between these three atoms form a coplanar trigonal structure.[28] Moreover, the hemiacetal is unstable and can react with the hydroxyl group again[29], resulting in an acetal with the same CH group attached to two –OR groups, as described in Fig. 2 E. These two chemical reactions make up the mechanism by which DAS is able to cross-link HLC with CS. Understanding these chemical principles was essential for HCD synthesis (Fig. 2 F). Therefore, via Schiff base and acetalization reaction could form covalent bonds between HLC, CS and HCD.

Swelling ratio analysis

Physiological saline was adopted as swelling media to mimic the body fluids to study their hydrolytic stability of the hydrogel when we place it into body fluids. As observed in Fig. 3(A), the swelling ratio of the hydrogels increased to the maximum value at 6h, When the time prolong to the 8h, the swelling ratio was not changed completely, and the swelling equilibrium was exhibited. The swelling ratio of HCD-1.0 is higher than that of other hydrogel, such as HCD-1.0 and HCD-1.5. With the content of DAS increased, the swelling ratio of hydrogels decreased. These results mainly due to the cross-linking agent play an important role in structure of hydrogels. The pore size of HCD-0.5 hydrogel is larger than HCD-1.5 and HCD-1.0 (Fig.5). The larger pore size could provide more space for fluids and water flow into hydrogels. Therefore, the swelling ratio of HCD-0.5 hydrogels is largest.

The mechanical strength analysis

As shown in Fig. 3 (B), the compression stress of HCD-0.5 (0.01 MPa) was higher than that of HCD-1.0 (0.005 MPa) and HCD-1.5 (0.0015 MPa) with the same compression displacement at 37°C. This can probably be ascribed to the influence of both structure and porosity on the flexibility and plasticity of the gel. The compression modulus (G) was directly proportional to compression stress; the better the flexibility of gel, the higher the compression modulus value. These results demonstrate that the more concentration of cross-linking agent (DAS contents), the lower strength of HCD hydrogels.

Biodegradation of HCD hydrogels *in vitro*

In order to assess the gamma rays may affect polymers and particularly soft samples of natural origin. So, the samples were sterilized by gamma irradiation or non-gamma irradiation. Firstly, the hydrogels are obtained in “aseptic conditions”, the weight loss of hydrogels were measured shown in Fig.3(C, D). The weight loss was decreased after degradation by physiological saline. The weight loss of HCD-1.5, HCD-1.0 and HCD-0.5 hydrogel were sterilized by non-gamma irradiation is 90%, 87% and 82%, while 90.5%, 87.5% and 82.5% were observed in HCD hydrogels were sterilized by gamma irradiation. The difference on the weight loss of HCD hydrogels sterilized by gamma irradiation or non-gamma irradiation is smaller, and even ignore. But these smaller differences may be contributing the operation processing produce the microorganism, which may consume or devour the HCD hydrogels.

Because of the body fluids contain the various enzymes such as collagenase class I, II, I+II etc., the HCD hydrogels injected into body (such as subcutaneous of mice) and would degrade by the body fluids. The HCD hydrogels were prepared for dermal filler, especially tissue repair. Therefore, we choose the collagenase class I, II, III to measure the degradation of HCD hydrogels. As *in situ* dermal fillers, the high biodegradation rate and poor biocompatibility couldn’t meet the demand *in vitro* and *in vivo* applications in many cases. As such, a hydrogel’s biodegradation rate should be evaluated *in vitro*. When the content of DAS in HCD hydrogels was higher, weight loss was slower (Fig. 4). The normalized residual weight (W_R) of HCD-1.5 was higher than that of the other HCDs at most time points. Moreover, from the results we determined that the biodegradation rates in the early stage (within 4 weeks) and the later stage (from 20 to 28 weeks) were higher than the biodegradation rate in the intermediate period (~4 to 20 weeks). For hydrogels degraded with class I collagenase (Fig. 4 A), the

W_R values of HCD-1.5, HCD-1.0, and HCD-0.5 were 61.78%, 58.28%, and 54.32%, respectively, at 28 weeks; those degraded by class II collagenase had W_R values of 56.92%, 52.8%, and 47.69% (Fig. 4 B), respectively, at 28 weeks. When class I and class II collagenase were used together, the resulting W_R values at 28 weeks were even lower, at 53.19%, 48.76%, and 42.19% (Fig. 4 C), respectively. The W_R value for HCD-0.5 at 28 weeks (42.19%), which was degraded with both types of collagenase, and represented the lowest W_R value of the study (Fig. 4 D).

Because collagenase can effectively degrade collagen *in situ* and remove the majority of proteoglycans and glycoproteins from collagens, it plays a key role in extracellular matrix dissociation.[30] In creating the HCD gels, when the number of hydroxyl and/or amino groups remains constant but the content of aldehyde groups increases, more covalent bonds form, resulting in stronger networks. Therefore, the W_R values of HCD-1.5 were higher than the W_R values of HCD-1.0 and HCD-0.5 at most time points. In the early stage of biodegradation, collagenase first degraded the proteoglycans and glycoproteins of HLC in the HCD hydrogels, and then they degraded the amino acid residues that did not participate in cross-linking. During the intermediate biodegradation period, the collagenase molecules had to permeate through the network to degrade the cross-linked amino acid residues, resulting in slowed degradation rates. In the later degradation period, previous enzymatic degradation left the network destroyed and exposed the residual amino acid residues to the collagenases, so the rate of degradation rose again in this phase.

While the above discussion explains the differing degradation rates over time, it does not explain why class I and class II collagenase degraded the HCD hydrogels at different rates. This observation was seen because collagenase performance depends on the degradation substrate; a specific collagenase may degrade one substrate faster than another substrate, given the substrates' differences in amino acid sequences and hydrolysis pathways, among other factors.[31] Class II collagenase displayed faster collagen degradation because the amino acid sequences on the HCD substrate were more suited to it than to class I collagenase. Moreover, because the sequence specificities for class I and class II collagenase are not only similar but are also complementary,[31] class I and II collagenase were able to synergistically degrade the HCD hydrogel such that the highest biodegradation rate was found when types of collagenase were used. Because the minimum W_R found in the entire study (for HCD-0.5 at 28 weeks) was only 42.19%, which involved degradation by both class I and class II collagenase, HCD may be a good material for creating long-term dermal fillers, although the time required for complete HCD degradation is still under investigation.

Morphology of HCD hydrogels

The hydrogel after lyophilisation and observed by SEM. A. Mikos et al.[32] reported that lyophilisation parameters may affect the porosity values. To support cell ingrowth and facilitate the exchange of nutrients and cellular waste products, *in situ* formed injectable scaffolds should possess highly porous networks with specified pore morphologies. In this respect, the most important parameters include pore size, porosity, and interconnectivity of the porous network. Pores with suitable diameters are essential for skin and tissue ingrowth because nutrients, oxygen, and waste must be able to diffuse through the pores to be carried to and from cells. Therefore, the hydrogel was lyophilised more than 48h during instance evacuation after freeze at -80℃, this good method is avoid to damage to structures of hydrogels. Scanning electron microscopy (SEM) images of the lyophilized HCD hydrogels (Fig. 5) confirmed that the hydrogel scaffolds have an open and interconnected porous structure. Pore sizes and cross-linking density varied with the concentration of DAS. Lower concentrations of DAS led to larger open holes in the hydrogels. Overall, the pore diameter distribution was between 30 and 60 μm. After 28 weeks of *in vitro* biodegradation, HCD hydrogels maintained their structural integrity and morphology even though the pore diameters after degradation were slightly larger than they were before degradation. Therefore, by examining the porous structure of the HCD hydrogels, we found that they contain a homogeneous distribution of stable and may support cell ingrowth.

Cytotoxicity of an extract solution from HCD hydrogels

As contact with cells correlation to structure of hydrogels, many chemicals may produce nonspecific alterations in cellular functions, resulting in toxicity. Therefore, detecting basal cytotoxicity *in vitro* by evaluating cells' ability to proliferate on the surface of a biomaterial is a necessary step before it is tested in an animal model. The results of the MTT assay, shown in Fig. 6, suggest that the relative growth rate (RGR) of cells varied with incubation time for all HCD hydrogel extract solutions. The RGR values increased dramatically at 5 days of incubation, where they peaked. The RGR values at 5 days of incubation were 115% for HCD-1.0 (50%) and 102% for HCD-0.5 (50%). RGR values at 7 days of incubation decreased slightly compared with those at 1, 3, and 5 days of incubation. The minimum RGR value throughout the experiment was 93% (HCD-1.5, 50%), which occurred at 7 days of incubation. From Fig. 6, it indicated that RGR values did not depend on the concentration of the extract solution. For example, RGR values for cells that received a low extract concentration (50%) were not always higher than the RGR values for cells receiving the high extract concentration (100%) at a given time point. In addition, when comparing the RGR values associated with different extract solutions throughout the experiment, there were no statistically significant differences relating to extract solution concentration or type ($P<0.05$).

In vitro tests are often performed to forecast the outcomes of or replace *in vivo* toxicity tests, and numerous studies have confirmed significant correlations between *in vitro* cytotoxicity and *in vivo* inflammatory responses.[33, 34] Because potentially dangerous chemicals are able to exert their effects at the cellular level, cytotoxicity assays are an effective means of predicting the acute phase response in animals.[35] Consequently,

in vitro cytotoxicity studies are generally performed before *in vivo* studies.

The results of the MTT evaluation (Fig. 6), indicate that RGR, regardless of extract solution and type, varied by incubation time. These results demonstrate that HCD was not cytotoxic under these preparation conditions because the more highly concentrated HCD extracts did not adversely affect cell growth. However, RGR values did fall below 100% at early incubation times (1 day and 3 days) because they were adjusting to the HCD particles present in the extract solutions, which may have influenced extracellular matrix production and the receptors that regulate cell growth.[34] By 7 days of incubation, the natural phenomenon of contact inhibition limited cell growth. While the minimum RGR during this experiment was 93% (7 days, HCD-1.5 50%), the maximum RGR was 115% (5 days, HCD-1.0 50%). RGR values over 100% indicate that the leaching solution was not cytotoxic, though whether or not the leaching solution was able to promote cell growth remains to be confirmed. Either way, biomaterials are considered to be safe for applications as long as RGR $\geqslant$ 90%, according to ISO 10993.5-2009.

Morphology of cells seeded onto HCD hydrogels

Cells were co-cultured with HCD hydrogels in 24-well culture plates so that cell growth occurred in direct contact with the hydrogels. The cell morphologies are shown in Fig. 7. Though a few cells were spherical, indicating that they had died and detached from the tissue culture dishes, the overwhelming majority of cells formed lamellipodia, were tightly attached, and became highly spindled after 1 day of incubation. After 3 days of incubation, the number of cells increased and individual cells grew larger. Moreover, a marked majority of cells joined together to form networks of interconnected cells, and nuclei were observed clearly. After 5 days of incubation, the number of cells continued to grow and individual cell sizes increased. The networks formed by interconnected cells were further enhanced, and cell clusters extended along a certain direction. Meanwhile, cell vitality remained high. At 7 days of incubation, cell numbers increased further, but individual cells appeared smaller and less vital as a result of contact inhibition. Fig. 7 shows that there were no differences in the quantity, size, and vitality of cells in contact with HCD-1.5, HCD-1.0, HCD-0.5, or cells in the control group.

Cytotoxicity from an implanted or injected biomaterial can arise as rapid-onset toxicity as well as delayed-onset toxicity. Therefore, both short-term and long-term studies are needed to thoroughly characterize a material's potential cytotoxicity. The most common and effective method for conducting long-term cytotoxicity tests involves exposing cells to the material for 24 hours or more before measuring the cell survival or proliferation.[36] As an implantable space-filling biomaterial, HCD hydrogels will be in contact with tissues for about 8 months, so this long-term cell attachment experiment is necessary for evaluating cell survival and proliferation. Compared with the control group, the quantity of cells co-cultured with HCD was not significantly different at any of the time points, but the morphologies of cells in the HCD groups were better because cells were larger and their nuclei were clearer. A qualitative biocompatibility assessment of the hydrogels demonstrated that cells can readily form three-dimensional (3D) cellular clusters on HCD hydrogels. The cell spreading onto the HCD hydrogels indicates that HCD hydrogels offer excellent biocompatibility and numerous adhesion sites. Moreover, there was no difference in cellular morphology and cell proliferation among the different HCD formulations (Fig.7). Therefore, HCD hydrogels seem to support cell survival and proliferation *in vitro*.

Histomorphometry near the injection site

The histocompatibility of a biomaterial, which determines its immunogenicity, is also important to its success *in vivo*. Based on histocompatibility assessments of foreign materials implanted in the body, biomaterials with excellent biocompatibility should show less intense immune responses or no material rejection. Moreover, short-term (within 12 weeks) and long-term (more than 12 weeks) investigations are needed to identify how the cell type and morphology of the tissue near the injected material changes with time. After cells are exposed to a subcutaneously delivered material, they change in the following ways: First, cell viability is enhanced within the first week of the material's introduction. Then in the transition period, biological or inflammatory reactions begin. In the late stage, the skin cells and connective tissue become stable state by 9-12 weeks after surgery, but this cycle is different for various animal species and materials.[35] As discussed above, the test period we chose for our study overlaps the time when biological and inflammatory reactions should achieve steady state after the operation. Consequently, in this study we analysed the histomorphometry and inflammatory responses the tissue around the injected materials at 1, 9, 12, and 28 weeks after the operation (Fig.8A).

As acute inflammation is the immediate response to foreign material, during which the interface between the blood and the material creates a series of alterations in the serum levels of several plasma proteins: serum amyloid A, C-reactive protein, fibrinogen, and alpha-1-antitrypsin.[37] In addition, changes in the microvasculature are also characteristic of this acute phase. Vessels first dilate and an excess of blood is available to the tissue near the foreign material.[38] Therefore, we used the quantity of vessels and blood volume as one way to assess the acute inflammatory reaction. The results shown in Fig. 8 B at 1 week suggest that none of the hydrogels tested caused a strong acute inflammatory response, given the small number of vessels and small amount of blood near the injection site. However, a few vessels covered the SUM gel at 9 weeks (Fig. 8 B (f)) after injection.

The chronic phase of the inflammation response is characterized by the proliferation of both fibroblasts and macrophages. Fibroblasts synthesize the collagen and proteoglycans necessary to encapsulate the implant and isolate it from the surrounding tissue.[39] Our results indicate that none of the gels were encapsulated by a fibrous capsule by 12 weeks

after the injection, but at 28 weeks HCD and SUM gels became encapsulated by a thin hyaline fibrous capsule (Fig. 8 B (d, h)). This natural response does not mean that these gels are unsuitable for use as filler biomaterials; capsule formation does not suggest poor biocompatibility.[40] However, the collagenous capsule does represent a barrier for transferring oxygen and nutrients within the hydrogel microenvironment and cell adhesion to the gel surface and fibrotic reactions are highly undesirable. For use as dermal filler though, the formation of a thin hyaline fibrous capsule will not hamper the use of HCD hydrogels.

The histomorphometry results for the HCD group were promising because they not only showed that HCD has a suitable colour and no adverse inflammatory responses, but it also possesses suitable mechanical strength and biological stability. Overall, HCD showed similar acute and chronic inflammation responses to those of SUM and EVL hydrogels.

Transmission electron microscopy (TEM) analysis

During implantation, or in our case injection, an interface is immediately created between the delivered material and the blood, whereby proteins from the blood and tissue fluid adsorb non-specifically to the material.[41] In this first step of the acute inflammatory response, proteins and phagocytes from the surrounding tissue cover the surface of the foreign material[42]. In the second step, the inflammatory reaction continues as microglial cells, macrophages, and foreign body giant cells wall off the implant, but the degree to which this happens depends on the material's characteristics and the implantation/injection site. These early inflammatory reactions constitute the acute phase response (APR), which can destroy or isolate the implanted system, but it can also lead to chronic inflammation. To determine the severity of the inflammatory response elicited by the HCD hydrogel, we evaluated a number of factors that signify inflammation: redness, edema, festering, the presence of blood vessels, the formation of a fibrous capsule, and the quantity of inflammatory cells present.

Shortly after the hydrogel injections (at 1 week), there were more inflammatory cells than there were at later times, and neutrophils were abundant. Moreover, the vitality of organelles such as the endoplasmic reticulum was also stronger shortly after implantation. These results indicate that the cells around the injection site were stimulated by the biomaterials within 1 week after they were delivered. The hydrogels induced only a slight inflammatory reaction, giving rise to a few neutrophils and others inflammatory cells. Nevertheless, of the amount of inflammatory cells associated with HCD was smaller than those associated with the SUM and EVL hydrogels, suggesting that HCD stimulated a less intense inflammatory response than the other hydrogels. In addition, while there were some fibroblasts and collagen fibers around the HCD gel, more fibroblasts and collagen were associated with the SUM and EVL hydrogels.

At 9 and 12 weeks after hydrogel delivery, the number of cells around the injection site remained steady and the inflammatory response transitioned into the chronic phase, characterized by the proliferation of both fibroblasts and macrophages. During this transition, the number of fibroblasts and collagen fibres increased and the number of inflammatory cells decreased. As shown in Fig. 9, in the later stage (28 weeks) after implantation, fibroblasts and collagen fibres were present and inflammatory cells were only found occasionally, indicating that a fibrous capsule had formed (this was supported by the histomorphometry analysis). Overall though, the number of inflammatory cells associated with the HCD gel was smaller at all times than those associated with the SUM and EVL gels.

Immunohistochemistry analysis

Injected polymers can induce specific immune system responses. First, the polymer can release various products by interacting with the surrounding tissue, and these products can bind to specific carriers and become antigens. Second, the proteins constituting the polymer or tissue proteins induced by the polymer can be treated as antigens, endocytosis, and then presented by an antigen-presenting cell (APC) to T cells.[26] For T cells to be stimulated, the foreign agents must be processed by APCs and complexes with a major histocompatibility complex (MHC) molecule (class II for CD4 lymphocytes; class I for CD8 lymphocytes) before being presented to surface lymphocytes.[39] Helper T cells (Th), which are also called CD4+ cells, assist humoral immunity and cellular immunity and are activated by reacting with polypeptide antigens presented by MHC II. CD8+ cells, which are cytotoxic T cells, are activated by reacting with polypeptide antigens presented by MHC I. CD68 exist on the surface of monocytes and macrophages, and they are glycoproteins that bind to low density lipoproteins. Because implanted biomaterials are potentially antigenic, the immunocompatibility of a new material must be considered before further biocompatibility testing.

To gain further insight into the inflammatory responses and demonstrate whether HCD had better histocompatibility compared with SUM and EVL, we performed an immunohistochemistry analysis of the skin tissue around the injection sites. Fig. 10 A, B, C represents the immunohistochemistry results for the HCD, SUM, and EVL hydrogels, respectively. As shown in Fig. 10 A, at 1 week the HCD group was stained by CD4, CD8, and CD68. CD4 stained the cytomembrane (Fig. 10 A (a)) light yellow, and CD8 stained the cytoplasm and nucleus light yellow, which appeared as a glandular tube (Fig. 10 A (e)). Fig. 10 A (i) shows extensive isabelline lesions where the cytoplasm and nucleus were stained by CD68. At 9 weeks after injection, the HCD-associated tissue was also stained a light yellow mesh by CD4 (Fig. 10 A (b)). However, CD8 did not stain the sample (Fig. 10 A (f)), and the area stained by CD68 was smaller than it was at 1 week (Fig. 10 A (j)). Compared with the assessment at 9 weeks, the 12-week HCD-associated samples showed a smaller area of CD4 staining. In addition, after 28 weeks the HCD-associated sections were not stained by CD4, CD8, or CD68 (Fig. 10 A (d, h, l)).

The results for the SUM and EVL hydrogels are described in Fig. 10 B, C, respectively. At 1 week (Fig. 10 B (a), Fig. 10 C (a)), CD4 stained extensive regions of the cytoplasm light

yellow, and CD8 stained extensive regions of cytoplasm and nucleus claybank (Fig. 10 B (e), Fig. 10 C (e)). Compared with Fig. 10 A (i), similar isabelline-stained lesions in the cytoplasm and nucleus, stained by CD68, were observed in Fig. 10 B (i) and Fig. 10 C (i). While the SUM samples were not stained by CD8 at 9 weeks, Fig. 10 C (f) shows a claybank area, suggesting that EVL was stained by CD8 at this time. From the remaining results, we found that most sections were not stained, except for the SUM (by CD4 and CD8) and EVL (by CD68) sections at 12 weeks.

In general, the immunohistochemistry results should be quantitative, so we assessed our results using both colour intensity and the density of positively stained cells. To determine the degree of the inflammatory reaction, we calculated these quantitative results, shown in Fig. 10D, using the following levels: no stain (—), slight satin (+; light yellow and small positive cell density), moderate stain (++; claybank and moderate positive cell density), strong stain (+++; isabelline and high positive cell density).

From Fig. 10D, it indicated that regardless of the injected hydrogel, the immune response intensity at 1 week was stronger than at later time points. For example, HCD-associated tissue was moderately stained (++) while the SUM and EVL gels produced strongly stained tissue (+++). While the degree of inflammatory responses lessened for all hydrogel groups at later times. Although the mechanism by which hydrogels induce antigens is not well understood, the following reasons may have contributed to our observed results: Shortly after injection, the surrounding tissue may not have been able to adapt to the hydrogels, so various products were secreted. These products may have bound to adequate tissue carriers and became antigens. However, the proteins constituting the hydrogels could have only become antigens once they were fully degraded. As time elapsed, the surrounding tissue may have adapted to the physical and chemical properties of the hydrogels, reducing the number of antigens released. Therefore, the immunohistochemistry reactions became weaker as time elapsed.

Conclusion

In this study, biologically stable and biocompatible HCD hydrogels were fabricated from human-like collagen and chitosan using dialdehyde starch as the cross-linker. The reaction mechanism involved the formation of convent bonds by acetalization and Schiff base reactions, and these bonds were confirmed by FTIR. The *in vitro* biodegradation investigation indicated that at least 42.19% of the HCD hydrogel was not degraded by collagenase after 28 weeks, suggesting good biological stability. The MTT and cytomorphology assays showed that HCD not only had no apparent cytotoxicity *in vitro* but it also supported cell growth on the hydrogel surface. Through histocompatibility evaluations, we found that HCD did not induce redness, edema, festering, or color changes; instead, it effectively filled the test regions, indicating good biological stability and adequate mechanical strength. In addition, compared with the SUM and EVL hydrogels, HCD induced less intense inflammatory responses. The good biological stability and biocompatibility of HCD, confirmed by a variety of *in vitro* and *vivo* evaluations in this study, indicate that HCD may be useful as dermal filler for cosmetic applications, so future studies will further examine the suitability of HCD hydrogels for use as dermal fillers.

Acknowledgments

This study was financially supported by the National Natural Science Foundation of China (21276210, 21106112, 201106111, 31000019, 21376190 and 21206135); the Shaanxi Provincial Scientific Technology Research and Development Program (2011JE003, 2012JQ2019, 2013KJXX-28, 2011JQ4026 and 2011JQ4026); China Postdoctoral Science Foundation (20110490171), and China Postdoctoral Science Special Foundation (2012T50815), the Scientific Research Program of Shaanxi Provincial Department of Education, China (2013JK0696, 12JS099, 12JS0100, and 12JS0101).

Notes and references

1 Shaanxi Key Laboratory of Degradable Biomedical Materials, School of Chemical Engineering, Northwest University, Xi'an 710069, China.
2 Shaanxi R&D Center of Biomaterials and Fermentation Engineering, School of Chemical Engineering, Northwest University, Xi'an 710069, China.
3 Shaanxi Provincial Institute of Microbiology, Xi'an 710020, China.
*Corresponding author: Daidi Fan: School of Chemical Engineering, Northwest University, Xi'an 710069, China. Tel.: +86-029-88305118; Fax: +86-029-88305118; E-mail address: fandaidi@nwu.edu.cn
§These authors contributed equally to this work.

1 J. S. Tememoff, A. G. Mikos, *Biomaterials*., 2000, 21, 2405–2412.
2 Q. Hou, A. Paul, K. M. Shakesheff, *J Mater Chem*., 2004, 14, 1915–1923.
3 M. Maeda, S. Tani, A. Sano, K. J. Fujioka, *Controlled Release*., 2010, 62, 313–324.
4 D. Wisser, J. Steffes, *Burns*., 2003, 29, 375–380.
5 E. B. Stephan, R. Renjen, S. E. Lynch, *J Periodontol.*, 2000, 71, 1887–1892.
6 J. D. Kakisis, C. D. Liapis, C. Breuer, B. E. Sumpio, *J Vase Surg*., 2005, 41, 349–354.
7 P. M. Taylor, S. P. Allen, S. A. Dreger, M. H. Yacoub, *J Heart Valve Disease*., 2002, 11, 298–306.
8 Y. E. Luo, D. D. Fan, X. X. Ma, D. W. Wang, Y. Mi, X. F. Hua, *Chin J Chem Eng*., 2005, 13, 276–279.
9 X. Li, X. X. Ma, D. D. Fan, C. H. Zhu. *Soft Matter*., 2012, 8, 3781–3790.
10 L. P. Jia, Z. G. Duan, D. D. Fan, Y. Mi, J. F. Hui, L. *Chang, Mater Sci Eng C*., 2013, 33, 727–734.
11 C. H. Zhu, D. D. Fan, Z. G. Duan, W. J. Xue, L. A. Shang, F. L. Chen, *J Biomed Mater Res Part A*., 2009, 89A, 829–840.
12 O. Felt, A. Carrel, P. Baehni, P. Buri, R. Gurny, *J Ocul Pharmacol Ther*., 2000, 16, 261–270.
13 J. Berger, M. Reist, J. M. Mayer, O. Felt, R. Gurny. *Eur J Pharm Biopharm*., 2004, 57, 35–52.

14 S. B. Ross-Murphy, *J Texture Stud*., 2007, 26, 391–400.
15 R. O. Beauchamp, M. B. G. St Clair, T. R. Fennell, D. O. Clarke, K. T. Morgan, F. W. Karl, *Crit Rev Toxicol*., 1992, 22, 143–174.
16 Q. Yang, F. D. Dou, B. Liang, Q. Shen, *Carbohydr Polym*., 2005, 59, 205–210.
17 X. F. Ma, J. G. Yu, N. Wang, *Macromol Mater Eng*., 2007, 29, 2723–2728.
18 J. F. Martucci, R. A. Ruseckaite, *J Appl Polym Sci*., 2009, 112, 2166–2178.
19 R. H. Wilson, *Proc Soc Exp Biol Med*., 1959, 102, 735–737.
20 X. Li, X. X. Ma, D. D. Fan and C. H. Zhu.et al. *Soft Materials*, 2014, 12, 1-11.
21 X. Li, D. D. Fan, J. J. Deng, et al. *Journal of Pure and Applied Microbiology*, 2013, 7(13), 475-480.
22 X. Li, D. D. Fan, J. J. Deng, et al. *Journal of Pure and Applied Microbiology*, 2013, 7(1), 359-364.
23 X. Li, D. D. Fan, J. J. Deng, et al. *Asian Journal of Chemistry*, 2013, 25(17), 9613-9616.
24 X. Li, X. X. Ma, D. D. Fan and C. H. Zhu.et al. *Journal of Materials Chemistry B*, 2014, 2, 1234-1249.
25 S. H. Pine, J. B. Hendrickson, D. J. Cram, G. S. Hammono, Organic chemistry.; McGraw-Hill: *New York*, 1980, 285–286.
26 T. W. G. Solomons, Organic chemical.; Wiley: *New York*, 1980, 703–714.
27 D. F. Williams, *J Mater Sci.*, 1987, 22, 3421–3445.
28 R. L. Gutman, G. Peacock, D. R. Lu, *J Controlled Release*., 2000, 65, 31–41.
29 H. Baumann, *J. Gauldie, Immunol Today*., 1994, 15, 74–80.
30 G. H. J. Wolters, G. H. Vos-Scheperkeuter, J. H. M. Van Deijnen, R. Van Schilfgaarde, *Diabetologia*.,1992, 35, 735–742.
31 M. D. Bond, H. E. Van Wart, *Biochem*., 1984, 23, 3085–3091.
32 A. Mikos, J. Temenoff, *EJB Electronic Journal of Biotechnology*, 2000, .3 (2), 1-6.
33 B. Ekwall. *Acta Pharmacol Sin*., 1983, 52, 80–99.
34 P. J. Guzzie, *New York*, 1994. 57–86.
35 J. W. Grisham, G. *J. Smith, Pharmacol Rev*., 1984, 36, 151–171.
36 E. Fournier, C. Passirani, C. N. Montero-Menei, J. P. Benoit. *Biomaterials*., 2003, 24, 3311–3331.
37 B. ŘÍhová, *Adv Drug Deivery Rev*., 1996, 21, 157–76.
38 B. ŘÍhová, *Adv Drug Delivery Rev*., 2000, 42, 65–80.
39 L. Tang, J. W. Eaton, *J Clin Pathol.*, 2004, 103, 466–471.
40 A. Remes, D. F. Williams, *Biomaterials*., 1992, 13, 731–43.
41 D. D. Fan, J. Y. Xing, W. J. Xue, C. H. Zhu, X. X. Ma, R. Ma, *Chin J Chem*., 2011, 29, 1811–1816.
42 D. D. Fan, *Chinese patent*., No. 01106757. 8, 2005.

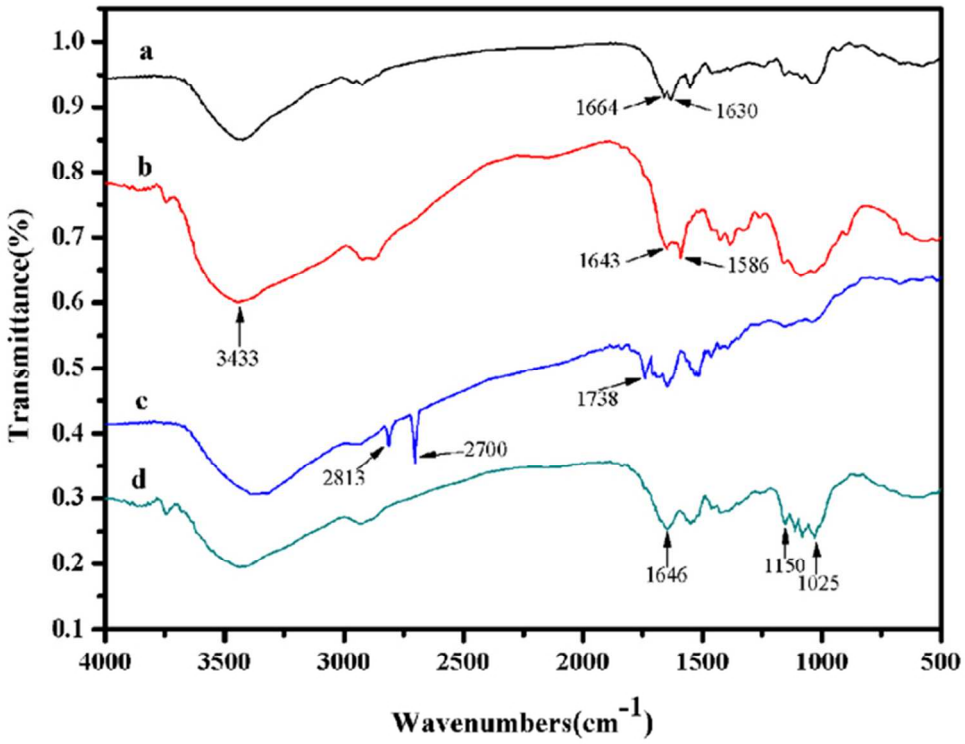

Fig. 1 FT-IR spectra of (a) macromer HLC, (b) CS, (c) DAS, and (d) HCD-1.0 hydrogel.
60x46mm (300 x 300 DPI)

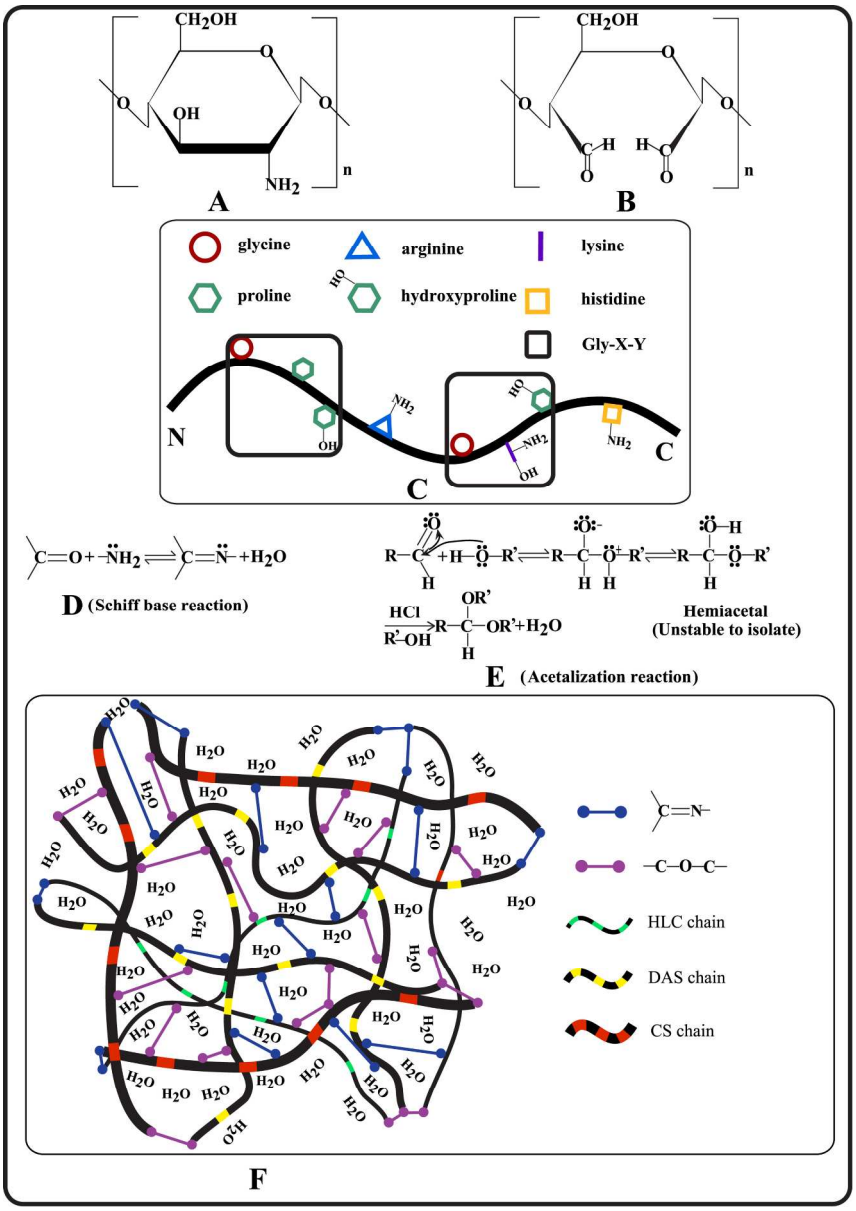

Fig. 2 Schematic illustration of HCD hydrogels synthesis: A, B is a monomer of the constitutional formula of chitosan (CS) and disaldehyde starch (DAS), respectively. C describes the basic structural module of Hum-like collagen (HLC) polypeptide chain. D, E is the Schiff base and Acetalization reaction, respectively, which were the main reaction principles forming covalent bonds in HCD hydrogels. F shows the 3-D structure of HCD hydrogels.
113x159mm (600 x 600 DPI)

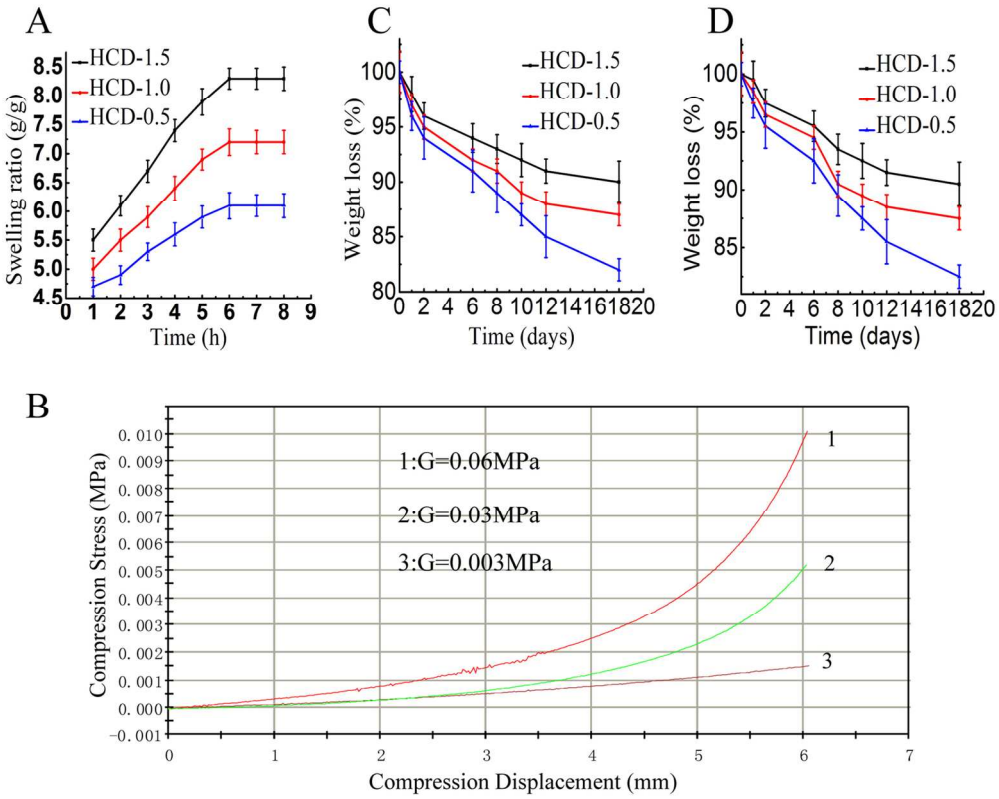

Fig. 3 (A) the swelling ratio of HCD hydrogels in physiological saline; (B) The relationship between compression stress and compression displacement: 1, HCD-0.5; 2, HCD-1.0; 3, HCD-1.5 hydrogels; (C) weight loss of HCD hydrogels were sterilized by non-gamma irradiation after degradation by physiological saline; (D) weight loss of HCD hydrogels were sterilized by gamma irradiation after degradation by physiological saline.
139x115mm (300 x 300 DPI)

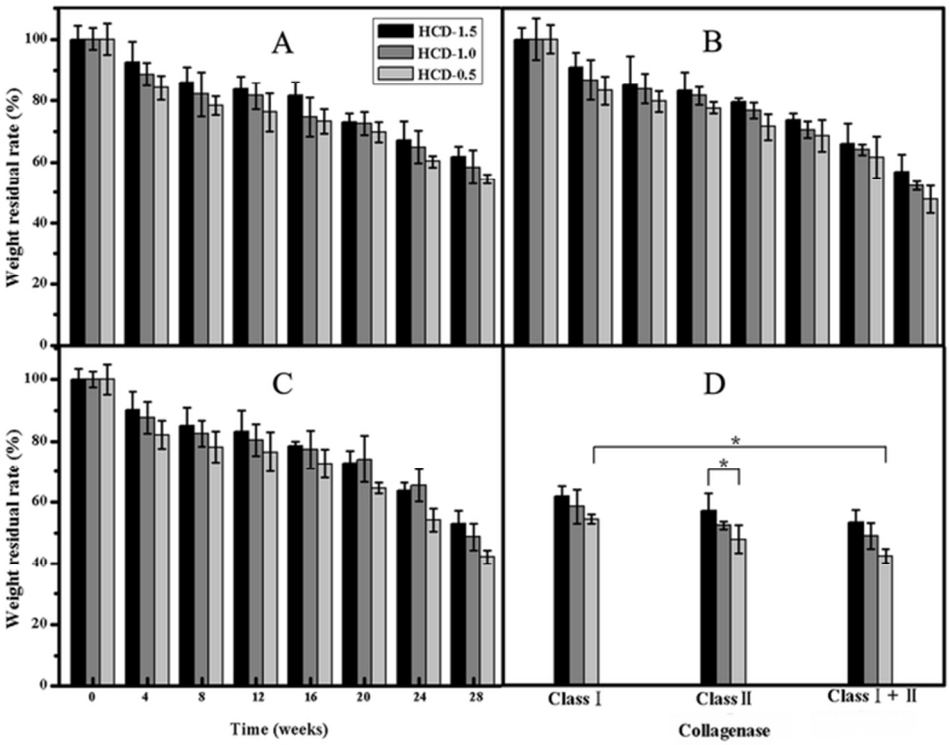

Fig. 4 The normalized residual weight (WR) of HCD hydrogels evaluated by collagenase (A) class I (100U/mL), (B) class II (100U/mL) and (C) class I + II (1:1 V/V). (D) The WR in various collagenases after 28 weeks degradation. *P＜0.05.
61x47mm (300 x 300 DPI)

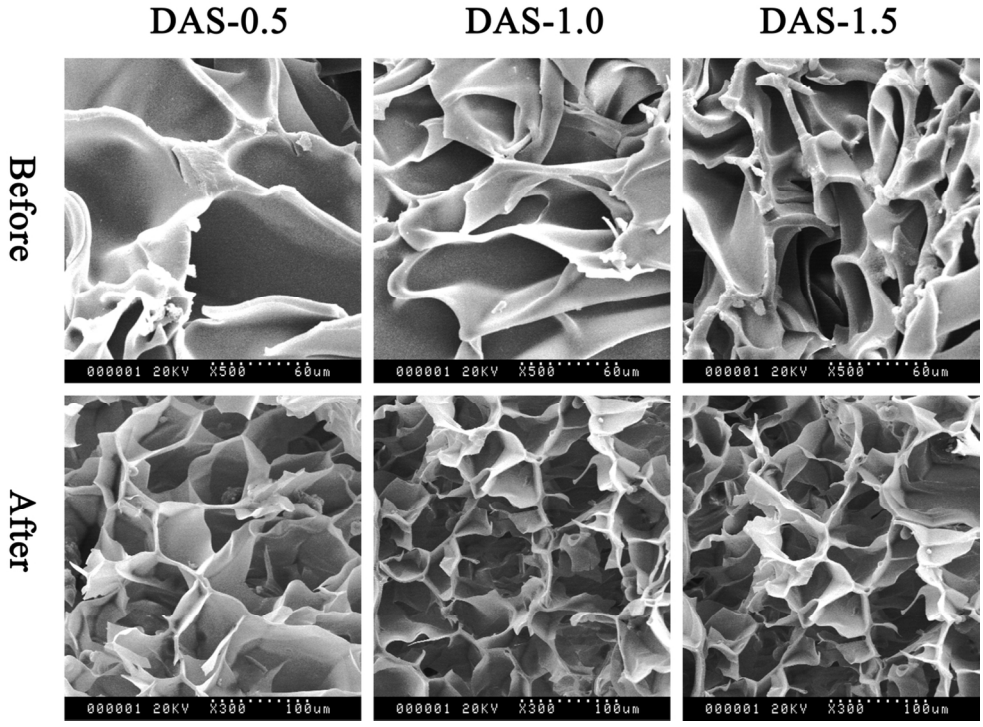

Fig. 5 The morphology of DAS hydrogels was evaluated by SEM. Before: assessment before biodegradation in vitro; After: assessment after 28 weeks biodegradation with collagenase.
59x43mm (600 x 600 DPI)

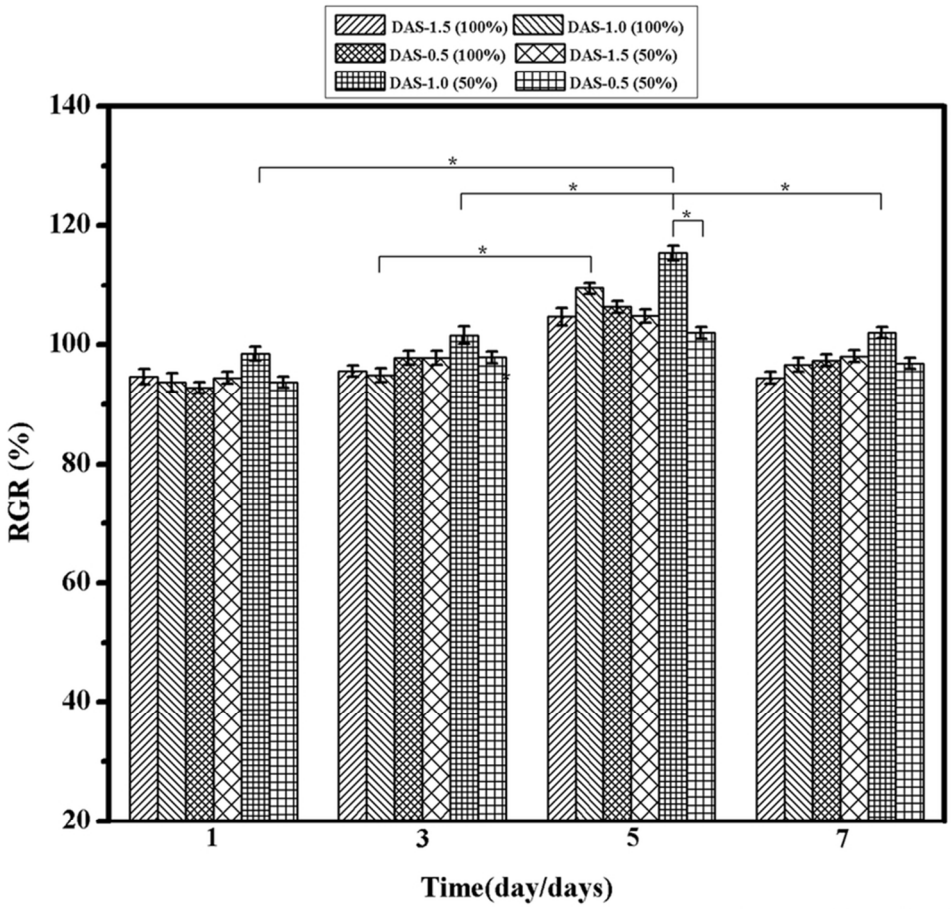

Fig. 6 The relative growth rate (RGR) of HCD hydrogels extract solution (100% and 50%), which was evaluated by MTT assay after 1 day, 3, 5, and 7 days incubation. *P＜0.05.
76x73mm (300 x 300 DPI)

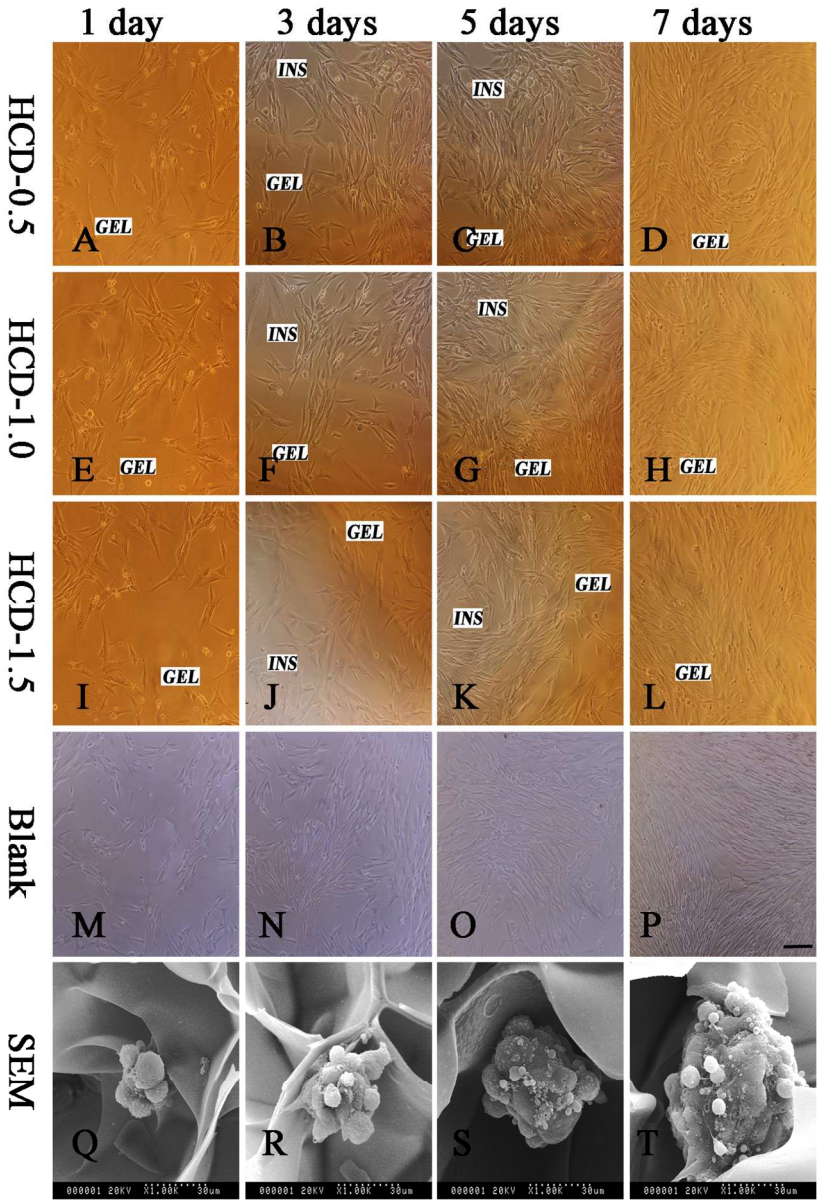

Fig. 7 The morphology of cells cultured with hydrogel. INS was the interspace between hydrogel and the well of 24-well culture plate where no hydrogel existed and appeared violet. GEL represented the HCD hydrogels which covered the cells and appeared orange. SEM: the cellular morphology in the DAS-1.0 hydrogel after incubation 1 day, 3, 5, and 7 days were evaluated by SEM. The control group, cells were cultured without hydrogel, appeared violet. Bar = 100 μm, (For interpretation of the references to colour in this figure legend, the reader is referred to the web version of this article).
113x163mm (299 x 299 DPI)

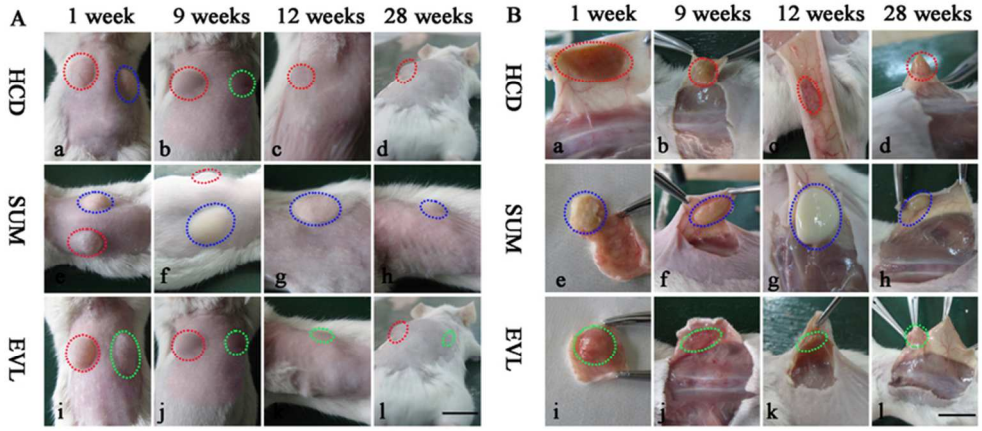

Fig. 8 The histomorphometry (A) and inflammatory responses (B) of HCD, SUM, and EVL were estimated in vivo. The results of HCD, SUM, and EVL at 1 week, 9, 12, and 28 weeks are described in (a, e, i), (b, f, j), (c, g, k) and (d, h, l), respectively. The red circle, blue circle and green circle represents the site where HCD, SUM, and EVL was injected into, respectively. Bar = 1 cm. (For interpretation of the references to colour in this figure legend, the reader is referred to the web version of this article).
74x34mm (300 x 300 DPI)

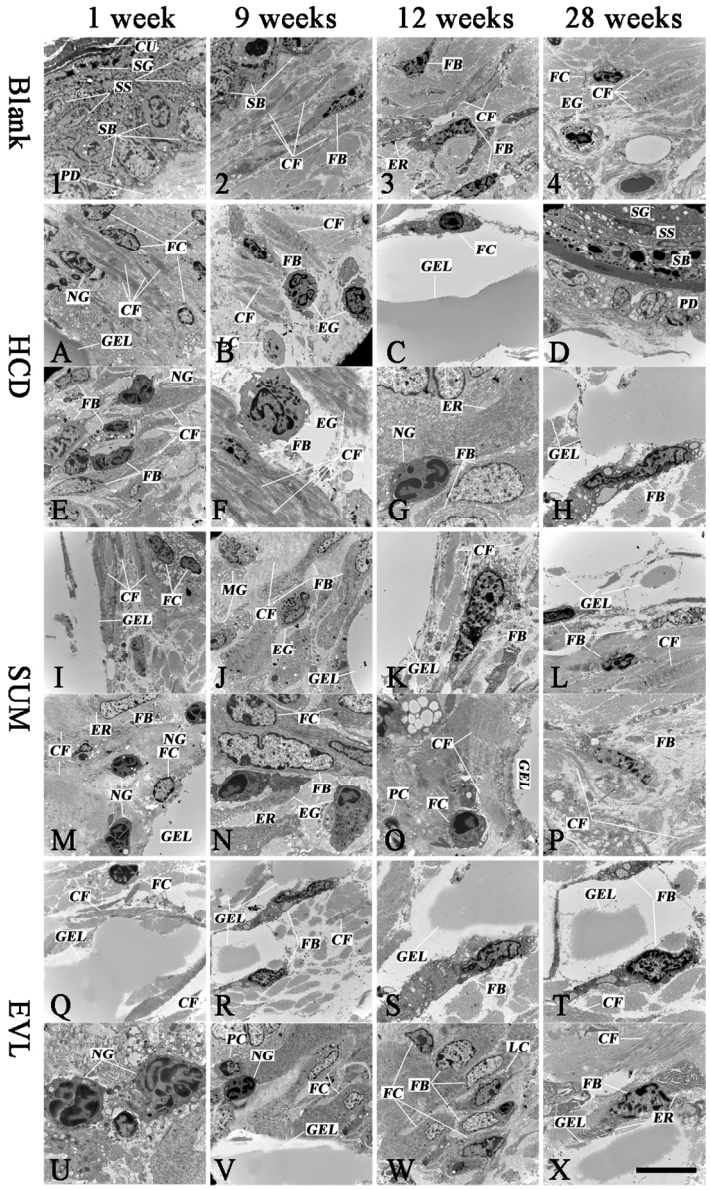

Fig. 9 The types and number of inflammatory cells of skin tissue around the injected site were evaluated by transmission electron microscopy (TEM). The results of HCD, SUM, and EVL at 1 week, 9, 12, and 28 weeks were described in ((A E), (I M), (Q U)), ((B F), (J N), (R V)), ((C G), (K O), (S W)) and ((D H), (L P), (T X)), respectively. Blank groups (1, 2, 3, 4), which represents the skin tissue where no hydrogel was injected into, were applied to compare with test groups (HCD) and control groups (SUM, EVL). Bar=5 μm. CU: cuticle, SG: stratum granulosum, SS: stratum spinosum, SB: stratum basale, PD: papillary dermis, CF: collagen fiber, FB: fibroblasts, ER: endoplasmic reticulum, FC: fibrocyte, EG: eosinophilic granulocyte, NG: neutrophils, LC: lymphocyte, MG: macrophages, PC: plasmocyte, GEL: the injected HCD, SUM, EVL gel, respectively.
142x230mm (199 x 199 DPI)

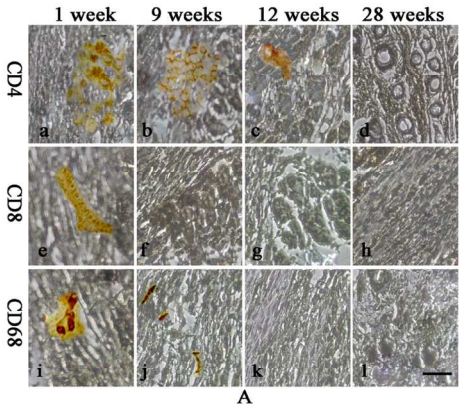

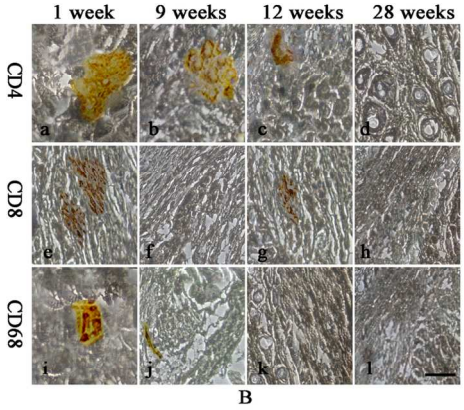

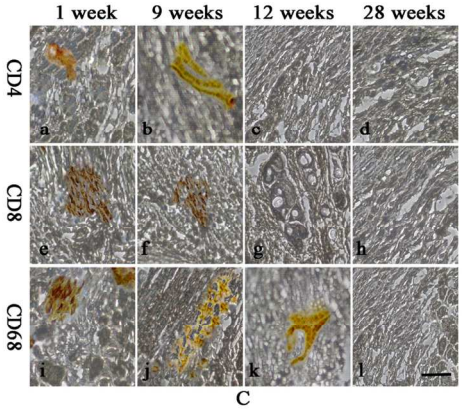

The quantitative results of immunohistochemistry analysis of HCD, SUM, and EVL skin tissue section.

		1 week	*9 weeks*	*12 weeks*	*28 weeks*
SUM	CD4	++	++	+	—
	CD8	++	—	—	—
	CD68	++	+	—	—
HCD	CD4	++	++	+	—
	CD8	+++	—	+	—
	CD68	++	+	—	—
EVL	CD4	++	++	—	—
	CD8	+++	++	—	—
	CD68	++	++	+	—

D

Fig. 10 Immunohistochemistry analysis of (A) HCD, (B) SUM, and (C) EVL sections which were stained by CD4, CD8, and CD68 after 1 week, 9, 12, and 28 weeks operation. (D) The quantitative results of immunohistochemistry analysis of HCD, SUM, and EVL skin tissue section. Bar=50μm. (For interpretation of the references to colour in this figure legend, the reader is referred to the web version of this article).
70x61mm (600 x 600 DPI)

The injectable, biodegradability, histocompatibility and biocompatibility of HCD hydrogels were determined through *in vitro* and *in vivo* tests.